# Adsorption on a stepped substrate

J. Merikoski and J. Timonen
*Department of Physics, University of Jyväskylä, P.O. Box 35, FIN-40351 Jyväskylä, Finland*

K. Kaski
*Tampere University of Technology, P.O. Box 692, FIN-33101 Tampere, Finland*
*and Research Institute for Theoretical Physics, P.O. Box 9, FIN-00014 University of Helsinki, Helsinki, Finland*
(Received 16 February 1994; revised manuscript received 24 May 1994)

The effect of substrate steps on the adsorption of particles is considered. The problem is formulated as a lattice-gas model with nearest neighbor interactions and it is studied by a numerical transfer-matrix method. In particular, the influence of the substrate-induced row potential on adsorbed monolayers is discussed. It is found that strong row-transition-like features appear in the presence of a row potential and it is suggested that these may be seen in adsorption on vicinal faces.

## I. INTRODUCTION

Adsorbed layers on solid surfaces have attracted considerable experimental, theoretical, and practical interest during recent years.[1–6] It is well known that substrate heterogeneities can have a major effect on the structure of adsorption layers and on adsorption kinetics.[2] Recently, the influence of substrate steps on phase transitions in adsorbed monolayers was studied theoretically by Albano *et al.*,[3] and a wetting transition in the limit of low step density was predicted. Experimentally deduced roughening transitions in adsorption systems have been reported by Larher and Angerand[4] for adsorption on flat substrates, and by Miranda *et al.*[5] for xenon on stepped palladium.

In this work we discuss the effect of the potential difference between adjacent adatom rows on adsorption on a stepped substrate. Experimental evidence of different types of adsorption sites has previously been found by measuring work function changes as a function of coverage in adsorption of hydrogen on stepped platinum substrates,[7] and in adsorption of xenon on stepped palladium.[8] In Ref. 9 these findings have been related to the existence of a substrate-induced row potential.

We shall be mainly concerned with the behavior of the adsorption layer on a terrace of a stepped substrate for temperatures well below $T_c$, the two-dimensional critical temperature of an adsorption layer on the corresponding flat substrate. At these temperatures the shape and the width of the interface between high-coverage and low-coverage phases are determined by the row potential. The results are obtained by numerically diagonalizing the transfer matrix of the two-dimensional Ising model with boundary conditions corresponding to adsorption of a monolayer on a single terrace of a stepped substrate. In addition, equilibrium Monte Carlo simulations have been used to check the results given by the transfer-matrix method, and to produce typical configurations of the model.

## II. THE MODEL

At low temperatures the adsorption of particles on each terrace of a stepped substrate is essentially independent of what is happening to the other terraces. Furthermore, below the roughening temperature of a flat face adsorption proceeds via a layer-by-layer mechanism so that practically no bulk excitations exist. We are thus led to study a strictly two-dimensional system with boundary conditions such that they correspond to a single step.

In order to describe adsorption on a terrace we use a two-dimensional lattice-gas model[10] with $L \times M$ geometry.[3] A schematic view of the substrate structure and the model is shown in Fig. 1. The Hamiltonian using the Ising formulation is given as follows:

$$\mathcal{H} = -\sum_{j=1}^{M}\Bigg[ J\sum_{k=1}^{L}\sigma_j^{(k)}\sigma_{j+1}^{(k)} + J\sum_{k=1}^{L-1}\sigma_j^{(k)}\sigma_j^{(k+1)} + H\sum_{k=1}^{L}\sigma_j^{(k)} + H_1\sigma_j^{(1)} + H_L\sigma_j^{(L)} + V\sum_{k=1}^{L}v(k)\sigma_j^{(k)}\Bigg], \tag{2.1}$$

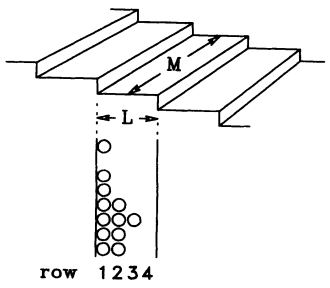


FIG. 1. Schematic view of a stepped substrate. In the transfer-matrix method we keep $L$ fixed and let $M \to \infty$.

 

where $\sigma_j^{(k)}$ is the occupation of the lattice site $j$ in the $k$th row parallel to the steps, with $\sigma_j^{(k)} = -1, +1$ for empty and occupied lattice sites, respectively. For $V = 0$ Eq. (2.1) yields the Hamiltonian used in Ref. 3, and with our choice for the boundary fields, $H_1 = -H_L = J = 1$, the step is wet at any finite temperature.[3,13,14] In our model an adatom in the $k$th row experiences an additional potential or row field proportional to $v(k)$, for which we have for simplicity chosen a *linear* dependence on the distance from the step edge,

$$v(k+1) = v(k) - 1 \quad \text{and} \quad v(1) = -v(L). \tag{2.2}$$

With the latter condition the layering "transition" point is $H = 0$, i.e., the coverage $\theta(H = 0) = 1/2$. For $V \geq 0$ the adsorption layer begins to grow from the step edge (row $k = 1$) as the value of the external field $H$ is increased. The influence of the form of the row potential and the relevance of our model to experimental systems will be discussed at the end of Sec. IV below.

In this work the unit of temperature is the critical temperature $T_c$ of the two-dimensional square-lattice Ising model,[12] $k_B T_c/J \approx 2.2692$. The correspondence between the Ising and lattice-gas variables is described in detail elsewhere.[15] With our sign conventions the chemical potential becomes $\mu = 2H - 8J$ and the coverage is given by $\theta = \frac{1}{2}(\mathcal{M} + 1)$, where the magnetization $\mathcal{M}$ is as follows:

$$\mathcal{M} = -\frac{1}{N}\frac{\partial F}{\partial H} = \frac{1}{L}\sum_{k=1}^{L}\langle\sigma_j^{(k)}\rangle. \tag{2.3}$$

The row coverages $\theta_k$ for each row $k$ are defined analogously. The susceptibility or the slope of the adsorption isotherms[4] is

$$\chi = \frac{\partial \mathcal{M}}{\partial H} = 4\frac{\partial \theta}{\partial \mu}. \tag{2.4}$$

In Fig. 2 snapshots of typical configurations of the model with $L = 4$ generated by Monte Carlo simulations[11] are shown. Even for a weak row potential ($V = 0.01$), the width of the interface between the high-coverage (+) and the low-coverage (−) phases will be substantially reduced by this potential, and the effect can be seen in a considerable temperature range, i.e., from zero temperature up to $T \approx 0.2T_c$. For increasing temperature, the meandering of the interface increases so that eventually the interface will extend over the whole terrace, and near $T_c$ isolated adatoms inside the (−) phase and vacancies inside the (+) phase will be generated. We choose the number of the adatom rows, $L$, to be an *even* number, and have, for the row potential defined by Eq. (2.2) with $V > 0$, a nondegenerate ground state (straight interface in the middle of the terrace) at $H = 0$. For odd $L$ the same results are found but for values of $H$ which are shifted by $V/2$.

Notice that the "row transitions" as discussed in this work are not real phase transitions, in contrast with the *layering transitions* in adsorption on flat substrates.[10] Therefore we use the term "row-by-row pseudotransitions" to describe the mechanism of the growth of a monolayer. At low temperatures the filling of a single adatom row happens essentially one dimensionally, but sharp transitions (for each row) occur only at zero temperature, which is the critical temperature of the one-dimensional Ising model.[12] Furthermore, there is a potential difference between *every* pair of adjacent adatom rows, and no true "delocalization transition" in the sense of Ref. 14 exists.

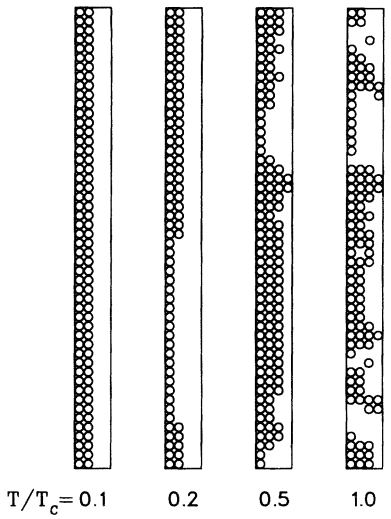


FIG. 2. Snapshots of lattice-gas configurations at $H = 0$ as generated by Monte Carlo simulations for $L = 4$ and $V = 0.01$. In each snapshot only a part of the simulation cell with $M = 200$ is shown.

## III. THE TRANSFER-MATRIX METHOD

At low temperatures the sampling of thermal fluctuations by the Monte Carlo method becomes exceedingly slow. Therefore we use the numerical diagonalization of the transfer matrix instead. The method of calculating exact thermodynamic averages by using transfer matrices is described in Ref. 12. Because our model consists of an infinite ($M \to \infty$) strip with a finite width ($L$ fixed), our system can be regarded as quasi-one-dimensional. The definition of the transfer matrix resembles in our case that of the one-dimensional Ising model,[12] with the exception that the state of the "site" $j$ is now described by a vector of Ising variables $\bar{\sigma}_j = (\sigma_j^{(1)}, \ldots, \sigma_j^{(L)})$, and the dimension of the transfer matrix is $2^L$. In this work the eigenvalues of the transfer matrix are computed numerically for step widths up to $L = 10$.

The partition function is obtained using the standard way with $Z_M = \mathrm{Tr}V^M \sim \lambda_1^M$ for $M \to \infty$, where $\lambda_1$ is the largest eigenvalue of the transfer matrix $V$. The coverage $\theta$, the row coverages $\theta_k$, and the susceptibility $\chi$ can be determined by differentiating the free energy $F = -k_B T \ln Z$ with respect to the appropriate fields. As for the one-dimensional Ising model,[12] the correlation length in the direction of the steps is given by $\xi = 1/\ln(\lambda_1/\lambda_2)$, where $\lambda_2$ is the second largest eigenvalue of $V$.

In order to calculate the structure factor $S(k)$ parallel to the step edges we use the result derived in the Appendix of Ref. 16,

$$S(k) = \sum_{s\neq 1} \frac{1-(\lambda_s/\lambda_1)^2}{1-2(\lambda_s/\lambda_1)\cos k + (\lambda_s/\lambda_1)^2} m_{1s}m_{s1} + 2\pi\delta(k)m_{11}^2, \tag{3.1}$$

where, for a symmetric transfer matrix,

$$m_{st} = \sum_i m_i x_{si} x_{ti}. \tag{3.2}$$

Here $x_{si}$ is the $i$th component of the the eigenvector associated with the eigenvalue $\lambda_s$ of the transfer matrix, and $m_i$ is the sum of $L$ spins in a site with configuration $i$. Notice that here a "site" means a row *across* a terrace, i.e., perpendicular to the step edges. Within our model no additional symmetries (cf. Ref. 16) can be used to further reduce the problem of calculating the structure factor. We are particularly interested in the half width at half maximum (HWHM), $W_{1/2}$, defined by $S(0) = 2S(W_{1/2})$, in which the $\delta$ peak, the second term on the right side of Eq. (3.1), is omitted.

At low temperatures and for $H = 0$ and $L$ even, many of our numerical results for quantities describing the fluctuations of the system (e.g., the susceptibility) are well approximated by the exactly known[12] behavior of the one-dimensional Ising model in an external field $B = V/2 > 0$. The reason for this can be easily understood by studying the lowest excitations that give the major contribution to the free energy. In this case the ground state is a straight interface, and at low $T$ a notable (but low) kink density is observed only in the two adatom rows in the middle of the terrace (rows $k = 2, 3$ for $L = 4$ in Fig. 2). Therefore these rows are well described by the one-dimensional Ising model with $B = +V/2$ for the row at $k = L/2$ and with $B = -V/2$ for the row at $k = 1 + L/2$, and they are nearly independent of each other because of the low kink density. Note that for these two rows the net effect from the couplings with the neighboring rows vanishes. For the one-dimensional Ising model it is easy to show, by using $\langle\sigma_0\sigma_r\rangle \sim \exp(-r/\xi)$, that

$$S\left(\frac{1}{\xi}\right) = \tfrac{1}{2}S(0) + O\left(\frac{1}{\xi^4}\right) \quad \Rightarrow \quad \xi \approx 1/W_{1/2}. \tag{3.3}$$

Notice that this result is exact for the Gaussian model.[17] As will be seen below, it holds well also for our model with $L$ rows defined by the complete Hamiltonian Eq. (2.1). We have also derived the average domain size $\langle l\rangle$ for the one-dimensional Ising model in an external field. For $B > 0$ it is the average size of $(-)$ domains inside the $(+)$ phase and, as shown in the Appendix, the result is

$$\langle l\rangle = (1-e^{-\gamma})^{-1}, \quad \text{where} \quad \gamma = \ln\lambda_1 + (B-J)/k_BT, \tag{3.4}$$

where $\lambda_1$ is again the largest eigenvalue of the transfer matrix. At low temperatures this quantity shows a behavior qualitatively similar to the correlation length $\xi$ and to the susceptibility $\chi$. Therefore the behavior of our model at low temperatures for $H = 0$ ($L$ even) is determined by the breaking of the kink-antikink symmetry, which results from an applied external field, i.e., $B$ for the one-dimensional model, and the row potential in our complete model. On the other hand, for $H = V/2$, e.g., the ground state is degenerate in the complete model: the row at $k = 1 + L/2$ has the same energy independent of whether it is empty or completely filled. At low temperatures this row can therefore be described by the one-dimensional Ising model in zero field.

## IV. RESULTS AND DISCUSSION

An example of the effects of the row potential on adsorption is provided by the adsorption isotherms of Fig. 3. These and all the other data presented in the figures of this section are computed for the complete Hamiltonian (2.1) by using the numerical transfer-matrix method as described above. Without the row potential, the adsorption layer seems to display sharp layeringlike features at low temperatures, as shown in Fig. 3(a). From such figures one may erroneously determine a "critical temperature" of the layering transition to be near $T = 0.1T_c$. This is a matter of scale and resolution, however, and the isotherms have in fact a finite slope at any finite temperature. The corresponding isotherms for a nonzero row potential are shown in Fig. 3(b). At low temperatures the behavior differs even more from that of a flat substrate: indeed, there is now a sequence of row-by-row pseudotransitions. As is evident from Fig. 3(b), for $V = 0.01$ the steps in the isotherms, caused by the row potential,

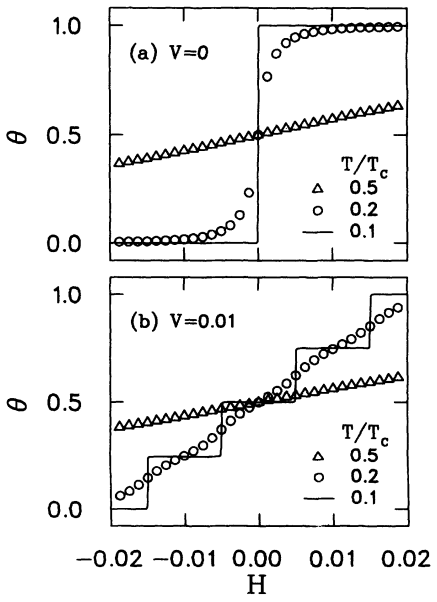


FIG. 3. Filling of the first adsorption layer on a stepped substrate with $L = 4$. Adsorption isotherms are shown for (a) $v = 0$ and (b) $v = 0.01$.

smear out near $T = 0.2T_c$. Even at this temperature, however, the slope of the isotherm near $H = 0$ is still much smaller than that in the case $V = 0$, Fig. 3(a). For higher temperatures the slopes in these two cases are very similar. The magnitude of the change in the slope of the $\theta$ vs $H$ curve is best seen by considering the behavior of the susceptibility as shown in Fig. 4, where the curves correspond to the coverage data shown in Fig. 3. By adding a row potential with strength $V = 0.01$, only one-hundredth of the nearest neighbor interaction between adsorbed atoms, the slope of the adsorption isotherms can be changed by several orders of magnitude. Notice how sharp the peaks may appear in the susceptibility although the true transition temperature is that of the one-dimensional Ising model, i.e., $T_c^{1D} = 0$.

The most interesting behavior for $V > 0$ is related to the plateaus between the row-by-row steps of the adsorption isotherms. Here we shall consider only the layering point at $H = 0$. In contrast with the case $V = 0$, the susceptibility is no longer a monotonic function of temperature at $H = 0$, as is evident from Fig. 5 which shows the susceptibility for two different strengths of the row potential and for a few step widths $L$. The susceptibility vanishes both at zero and infinite temperature, $\chi(T \to 0) = \chi(T \to \infty) = 0$, and a maximum occurs near a temperature $T = T_r$. Above $T_r$ the behavior of the system is not dominated by the row potential. The maximum value of the susceptibility, $\chi_{max}(H = 0) = 2/LV$, can be directly determined from Fig. 3 by noting that the interval between the row-by-row pseudotransitions in the $H$ scale is $V$. For strengthening row potential the row-by-row mechanism prevails at higher temperatures. For increasing $L$ the determination of $T_r$ from the susceptibility curves becomes more difficult: for $V = 0.01$ and

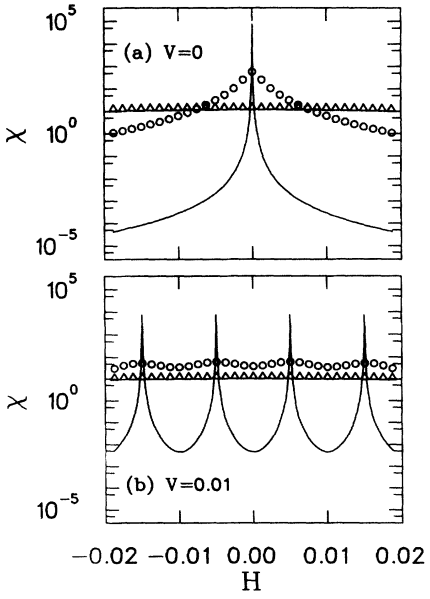


FIG. 4. The slope of the adsorption isotherm, or the susceptibility $\chi$, as a function of $H$ for three different temperatures for (a) $V = 0$ and (b) $V = 0.01$ with $L = 4$. The plotting symbols are the same as in Fig. 3.

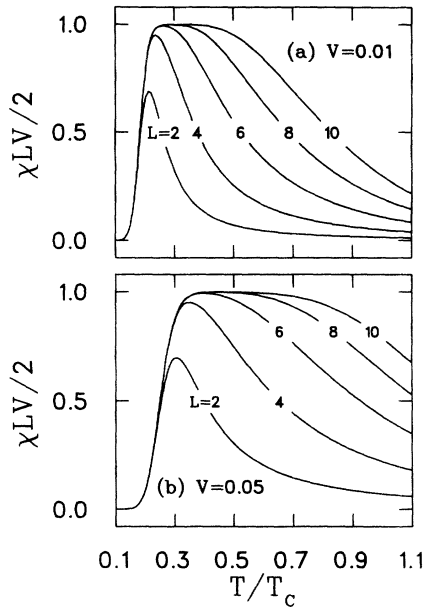


FIG. 5. The susceptibility $\chi$ for (a) $V = 0.01$ and (b) $V = 0.05$ at the layering transition point $H = 0$.

$L = 10$, e.g., the susceptibility is practically constant for $0.25 < T/T_c < 0.45$. The plateau in the susceptibility is in fact an evidence of the row potential.

More detailed information is gained by studying the row coverages, some of which are shown in Fig. 6. At $T = 0.2T_c$ the adatom layer grows by the row-by-row mechanism, which can also be seen as a slight modulation of the susceptibility in Fig. 4(b). At $T = 0.5T_c$ these pseudotransitions are no longer visible. The form of the $\theta_k = \theta_k(H)$ curves for the rows in the middle of the terrace is practically independent of $L$, and at $T = 0.2T_c$

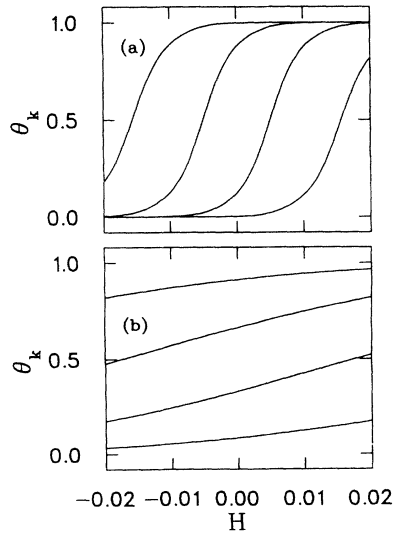


FIG. 6. Row coverages $\theta_k$ of adatom rows $k$ for a system with $L = 4$ and $V = 0.01$ for (a) $T = 0.2T_c$ and (b) $T = 0.5T_c$. The curves from top to bottom show the data for $k$=1, 2, 3, and 4, respectively.

we find $\theta_{L/2}(H=0) = 1 - \theta_{1+L/2}(H=0) \approx 0.9$. Thus we can conclude that for $L \geq 4$ the basic mechanism of filling of the adsorption layer is independent of the step width $L$, and, therefore, the temperature $T_r$ should be determined from that part of the susceptibility curve which is independent of $L$. Then at $H = 0$ for $T < T_r$ the behavior of a single row can be in excellent approximation described by that of the corresponding one-dimensional Ising model (see Sec. III).

The HWHM $W_{1/2}$ (solid curves) and the correlation length $\xi$ (plotting symbols) as a function of temperature for $H = 0$ are shown in Fig. 7. The result (3.3), which has been derived for the one-dimensional Ising model, is found to be valid for our model with several rows. Note that $\xi$ is the correlation length for fluctuations and not a measure of order in the system. Only for $V = 0$ (or $B = 0$ in the one-dimensional Ising model) is it directly connected with the kink density. Drawing on the analogy with the one-dimensional Ising model, we also show in Fig. 7 (dotted line, $V = 0.1$) the quantity $\rho' = -1/\ln(1-2\rho)$, where $\rho$ is the kink density. The kink density $\rho$ is a monotonic function of temperature and for $V \ll J$ depends only weakly on the strength $V$ of the row potential. In the scale of Fig. 7, $\rho'$ for $V = 0.01$ (and $V = 0$) is indistinguishable from the $1/W_{1/2}$ curve for $V = 0$. The kink density $\rho$ measures short-range order, and, therefore, for $V > 0$, $\rho'$ provides a good approximation for $\xi$ only at high temperatures. At low temperatures order is induced by the row potential.

In Fig. 8 we show the inverse of the HWHM as a function of $H$. Notice that the form of the row potential $v$ can be directly deduced from Fig. 8. For a linear row potential like the one in Eq. (2.2), at low temperatures the maxima in $1/W_{1/2}$ are equally spaced as a function of $H$. The temperature $T_r$, below which the width of the interface between the high-coverage and low-coverage phases is noticeably reduced, obviously depends only on the potential *difference* between two adjacent adatom rows on the terrace. Therefore, for a more complicated form of

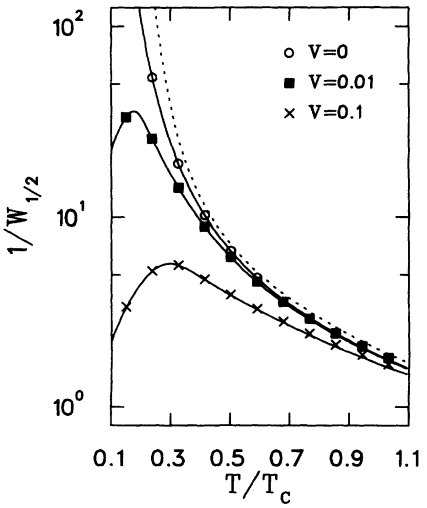


FIG. 7. The inverse HWHM of the structure factor, $1/W_{1/2}$ (solid curves), and the correlation length $\xi$ (plotting symbols) as a function of $T$ for $L = 4$ and at $H = 0$.

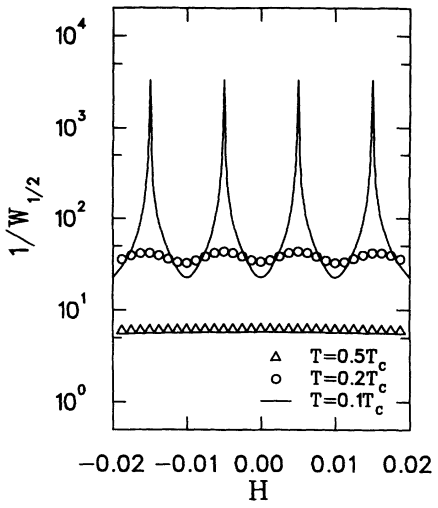


FIG. 8. The inverse HWHM of the structure factor, $1/W_{1/2}$, as a function of $H$ for three temperatures and for $L = 4$, $V = 0.01$.

the row potential, the definition of $T_r$ will not be unique, and it should be defined separately for each pair of rows. Moreover, different quantities, e.g., $\chi$, $\xi$, $\langle l \rangle$, etc., would give slightly different temperatures for the disappearance of the effects induced by the row potential. This of course reflects the fact that no real phase transition is involved. The influence of the nonlinearity of the row potential in real physical systems is thus twofold: the row-by-row pseudotransitions will not be equally spaced on the chemical potential axis, and the effects induced by the row potential will disappear at a temperature that depends on the coverage.

We have seen above that even a weak potential difference, $\Delta V(k) = |V(k) - V(k-1)|$, between two adjacent rows at $k$ and at $k-1$ can have a considerable effect on such physical quantities as are related to thermal fluctuations. In the case which we have considered here, $\Delta V(k) \equiv V$, this effect has been shown to be noticeable for $V$ as small as $V = 0.01$, at least for temperatures up to $T = 0.2T_c$. In Ref. 9 a row potential $V(k) = V(1)/k^3$ was used. In that case $\Delta V(k) > 0.01$ for rows up to $k = 4$ if $V(1) = 1$, and up to $k = 7$ if $V(1) = 5$; the latter value for $V(1)$ being the parametrization used[9] to reproduce the experimentally observed work function changes for the systems Xe/Ru(0001) and Xe/Pd[8(100)×(110)]. We can conclude that the behavior described in this work can be observed in experimental systems with more complicated row potentials, provided that our model defined by the Hamiltonian (2.1) otherwise contains the physical interactions relevant to the structure of the adsorption layer. The most obvious candidates for such experimental systems are given by adsorption of rare gas atoms on stepped metal substrates, such as Xe on Pd[8(100) × (110)] studied in Refs. 5 and 8. The observed[8] binding energies of adatoms at step sites (row 1) and terrace sites suggest that, for this system, our choice of strong boundary fields is justified (see also Ref. 3). In fact a simple bond-counting argument shows that the condition $H_1 \geq J$ is essential for the row-by-row mechanism to exist, and that this condition must be appropriately modi-

fied for adsorption layers with a structure different from the square lattice used in this work. We do not expect the parameters of our nearest neighbor lattice-gas model with pairwise interactions to have a simple correspondence with the measured *heats of adsorption* for rare gases, but we do think that the qualitative picture given by the model of the influence of the row potential on the structure of the adsorption layer is correct. Obviously, a well-characterized substrate with equally spaced steps is needed for detecting sharp row-by-row pseudotransitions in experiments. For the adsorption of rare gas atoms on a metal substrate, the characteristic excitation energies for the substrate are much larger than those for the adsorbate and, therefore, the kink density in the substrate steps is very small at low (in the energy scale of the adsorbate) temperatures. For a substrate with regularly kinked steps, such as the ruthenium surfaces of Ref. 18, the adatom rows cannot be reasonably defined, and a more complicated behavior is expected.

Our model was defined to describe an adsorbed *monolayer* on a stepped substrate, but it has some relevance to the growth of multilayers at low temperatures, for which adsorption proceeds via a layer-by-layer mechanism. For the second layer, there also exists a boundary field $H_1$ with a magnitude of the order of the nearest neighbor interaction $J$, but now this boundary field is not induced by the substrate step alone: there are in addition interactions with the adatoms in row $L$ of the first complete adsorption layer. The strength of this boundary field for the second and further layers is highly dependent on the geometry of the system, and on the relation between the lattice constants of the substrate and the adsorbate. Also the substrate potential for these layers is expected to be row dependent, due to the orientation of the terraces with respect to the high-indexed face. In fact, the linear approximation of Eq. (2.2) for the form of the row potential gets better when the distance from the substrate increases. In the experiments of Ref. 5, unexpectedly low estimates for the critical temperatures of the layering transitions on a stepped substrate were reported. We think that this observation may be (through the limited accuracy of the vapor pressure axis) a consequence of the rounding of the adsorption isotherms, a phenomenon we explained while discussing Figs. 3 and 4. Note that the existence of steps alone (with zero row potential) is sufficient for this rounding to occur and, strictly speaking, no sharp layering transitions exist on vicinal substrates. However, at temperatures well below the $T_c$ of the adsorption layer on a corresponding flat substrate, the substrate-induced row potential should have a profound effect on the formation of each layer in a multilayer system. It would be of interest to seek for an experimental verification of this hypothesis for this[5] or a similar adsorption system.

## V. CONCLUSIONS

The influence of a row potential on adsorbed monolayers on a stepped substrate has been studied in the framework of a lattice-gas model with $L \times M$ geometry with $M \to \infty$ and fixed $L$. We have considered here the model with strong boundary fields, i.e., the case for which the step without the row potential would be *wet* already at zero temperature. For simplicity we assumed a linear dependence of the row potential on the distance of the row from the step edge. Numerical diagonalization of the transfer matrix was found to be the most efficient method for analyzing the model at low temperatures.

We have shown that if even a weak row-dependent potential is included in the model, the behavior of the adsorption layer can be drastically changed for a temperature range which is an order of magnitude larger than the strength of the row potential. This effect is qualitatively understood by introducing the concept of row-by-row pseudotransitions, and it can be quantitatively measured by studying the behavior of the structure factor in the direction parallel to the step edges. The HWHM of the structure factor shows behavior similar to that of the slope of the adsorption isotherms or the susceptibility, and this behavior can be directly related to the existence and to the form of the row potential. At low temperatures, the fluctuations of the system turn out to be well described by the corresponding quantities in the one-dimensional Ising model, which reflects the one-dimensional nature of the formation of each adatom row. To experimentally observe the oscillations in the susceptibility as a function of the chemical potential, a high resolution of the chemical potential is obviously required. With a row potential proportional to $1/k^3$, where $k$ is the row number, these measurements should be feasible at least for a few innermost adatom rows, for which the potential difference between adjacent adatom rows is non-negligible.

## ACKNOWLEDGMENTS

This work has been supported by the Academy of Finland. Part of the computations were performed on Cray X-MP at the Center of of Scientific Computing (CSC) in Espoo, Finland.

## APPENDIX

In this Appendix the derivation of Eq. (3.4) for the average domain size in the one-dimensional Ising model is outlined. The Hamiltonian is given by[12]

$$\mathcal{H}_{1D} = -J\sum_{j=1}^{M}\sigma_j\sigma_{j+1} - B\sum_{j=1}^{M}\sigma_j, \tag{A1}$$

where $\sigma_j$ are Ising variables with $\sigma_j = \pm 1$, $B$ is the external magnetic field, and periodic boundary conditions $\sigma_1 \equiv \sigma_{M+1}$ are imposed. First we need to calculate the probability $P_+(l)$ for the length of a $(-)$ domain inside the $(+)$ phase to be $l$,

$$P_+(l) = \frac{P(\sigma_M = +1, \sigma_1 = \sigma_2 = \cdots = \sigma_l = -1, \sigma_{l+1} = +1)}{P(\sigma_M = +1, \sigma_1 = -1)}, \tag{A2}$$

where the two probabilities $P$ obey the equilibrium distribution $P(\{\sigma_j\}) \propto \exp[-\mathcal{H}_{1D}(\{\sigma_j\})/T]$ with $k_B = 1$. Here $B > 0$ is assumed; for $B < 0$ the signs are reversed. By defining two-dimensional matrices $S$ and $T$ by $S_{ij} = \delta_{i1}\delta_{1j}$ and $T_{ij} = \delta_{i2}\delta_{2j}$, Eq. (A2) reads as follows:

$$P_+(l) = \frac{\mathrm{Tr} SV(TV)^l SV^{M-l-1}}{\mathrm{Tr} SVTV^{M-1}}, \tag{A3}$$

where $V$ is the transfer matrix

$$V = \begin{pmatrix} e^{(J+B)/T} & e^{-J/T} \\ e^{-J/T} & e^{(J-B)/T} \end{pmatrix} \tag{A4}$$

with eigenvalues

$$\lambda_{1,2} = e^{J/T}\cosh(B/T) \pm [e^{2J/T}\sinh^2(B/T) + e^{-2J/T}]^{1/2}. \tag{A5}$$

The denominator of the right side of Eq. (A3) simply gives the unnormalized kink density, and the numerator can easily be evaluated since in the matrix $TV$ the elements of the top row are zero. After extracting the product $(TV)^l$, the traces are calculated in the usual way[12] by using the similarity transformation that diagonalizes $V$ to $V_{\mathrm{diag}} = \mathrm{diag}(\lambda_1, \lambda_2)$. For large $M$ the denominator of the right side of Eq. (A3) behaves as $\sim \lambda_1^{M-2}$ and the numerator as $\sim \lambda_1^{M-l-2} e^{l(J-B)/T}$. Thus $P_+(l) \propto e^{-\gamma l}$ and the average domain size is the sum $\langle l \rangle = \sum_l l P_+(l) = 1/(1 - e^{-\gamma})$, where $\gamma$ is defined in Eq. (3.4). Note that other quantities, e.g., magnetization for the one-dimensional Ising model and row coverages for the complete Hamiltonian (2.1), can be expressed in a similar way as a trace of a suitable combination of operators, instead of differentiating the free energy.


[1] *Phase Transitions in Surface Films*, edited by J. G. Dash and J. Ruvalds (Plenum, New York, 1980); *Kinetics of Ordering and Growth at Surfaces*, edited by M. G. Lagally (Plenum, New York, 1990).

[2] For reviews of adsorption on stepped surfaces, see H. Wagner, in *Solid Surface Physics*, edited by G. Höhler (Springer, Berlin, 1979); K. Wandelt, Surf. Sci. **251/252**, 387 (1991).

[3] E. V. Albano, K. Binder, D. W. Heermann, and W. Paul, Z. Phys. B **77**, 445 (1989); Surf. Sci. **223**, 151 (1989); J. Chem. Phys. **91**, 3700 (1989).

[4] Y. Larher and F. Angerand, Europhys. Lett. **7**, 447 (1988).

[5] R. Miranda, E. V. Albano, S. Daiser, K. Wandelt, and G. Ertl, J. Chem. Phys. **80**, 2931 (1984).

[6] D. Zhu and J. G. Dash, Phys. Rev. Lett. **57**, 2959 (1986); M. Sokolowski and H. Pfnür, Phys. Rev. Lett. **89**, 183 (1989); R. Gangwar and R. M. Suter, Phys. Rev. B **42**, 2711 (1990).

[7] K. Christmann and G. Ertl, Surf. Sci. **60**, 365 (1976).

[8] R. Miranda, S. Daiser, K. Wandelt, and G. Ertl, Surf. Sci. **131**, 61 (1983).

[9] E. V. Albano and H. O. Mártin, Phys. Rev. B **35**, 7820 (1987); **38**, 7932 (1988).

[10] M. J. de Oliveira and R. B. Griffiths, Surf. Sci. **71**, 687 (1978); R. Pandit, M. Schick, and M. Wortis, Phys. Rev. B **26**, 5112 (1982).

[11] See, e.g., *Monte Carlo Methods in Statistical Physics*, edited by K. Binder (Springer, Berlin, 1979).

[12] R. J. Baxter, *Exactly Solved Models in Statistical Mechanics* (Academic Press, London, 1982).

[13] G. Gallavotti, Riv. Nuovo Cimento **2**, 133 (1972).

[14] D. B. Abraham, Phys. Rev. Lett. **44**, 1165 (1980).

[15] M. Toda, R. Kubo, and N. Saitô, *Statistical Physics I* (Springer, Berlin, 1983).

[16] N. C. Bartelt and T. L. Einstein, J. Phys. A **19**, 1429 (1986).

[17] S. Ma, *Modern Theory of Critical Phenomena* (Benjamin, Reading, MA, 1976).

[18] A. Jablonski and K. Wandelt, Surf. Sci. **251/252**, 650 (1991).